IEEE Access
Multidisciplinary | Rapid Review | Open Access Journal

Received September 8, 2020, accepted September 23, 2020, date of publication October 1, 2020, date of current version October 19, 2020.

Digital Object Identifier 10.1109/ACCESS.2020.3028145

A Robust Random Noise Suppression Method for Seismic Data Using Sparse Low-Rank Estimation in the Time-Frequency Domain

PINGPING BING[1], WEI LIU[2], AND ZHIHUA ZHANG[2]
[1]Academician Workstation, Changsha Medical University, Changsha 410219, China
[2]College of Mechanical and Electrical Engineering, Beijing University of Chemical Technology, Beijing 100029, China

Corresponding author: Pingping Bing (bpping@163.com)

This work was supported by the Project of Scientific Research Fund of Hunan Provincial Education Department under Grant 19C0185.

ABSTRACT The noise separation from seismic data is of significant importance in geophysics. In most cases, the random noise always overlaps the seismic reflections over time, which makes it challenging to suppress. To enhance seismic signal, we propose a robust noise suppression method based on high-order synchrosqueezing transform (FSSTH) and robust principal component analysis (RPCA). Firstly, the noisy seismic data is transformed into a sparse time-frequency matrix (TFM) using the FSSTH. Then, the RPCA algorithm is employed to decompose the sparse TFM into a low-rank matrix and a sparse matrix that can be used to depict the useful signal and noise, respectively. Finally, the denoised signal can be obtained by back-transforming the low-rank matrix to the time domain via the inverse FSSTH. We utilize a synthetic data and two field datasets to demonstrate the robustness and superiority of our method, and compare with the conventional denoising algorithms such as $f-x$ denconvolution and $f-x$ singular spectrum analysis (SSA). The obtained results indicate that the proposed method is capable of achieving an excellent tradeoff between random noise suppression and seismic signal preservation.

INDEX TERMS High-order synchrosqueezing transform, robust principal component analysis, low rank matrix, noise suppression.

I. INTRODUCTION

During the field data acquisition, seismic signal is always accompanied by a great deal of noise. Random noise is one of the most common types of the seismic noise, which is often characterized by random oscillations and covers the seismic reflections throughout the time [1]. This brings great difficulties to the follow-up analysis and interpretation of seismic records. Therefore, improvement of the signal-to-noise ratio (SNR) is the primary task in the processing of geophysical data [2]–[4].

In recent decades, a large number of methods have been introduced for seismic random noise reduction. The widely used algorithm is the prediction-based method such as $f-x$ deconvolution [5], $t-x$ predictive filtering [6], non-stationary predictive filtering [7], and forward-backward prediction approach [8]. Such techniques take full advantage of the predicable property regarding seismic signal along spatial direction to design prediction filter for identifying the useful signal and the noise. Decomposition based algorithm is another type commonly used noise suppression method, which usually decomposes the noisy seismic data into a series of components and then the signal and noise can be separated based on their time and frequency difference. Empirical mode decomposition (EMD) [9], [10] and its extensions, e.g. ensemble empirical mode decomposition (EEMD) [11], complete ensemble empirical mode decomposition (CEEMD) [12], [13], have been successfully applied to seismic noise reduction [14]. Variational mode decomposition (VMD) [15] was first proposed by Dragomiretskiy and Zosso as an alternative to replacing EMD because of its robustness to sampling and noise, and it has been used for noise removal in [16]. Regularized non-stationary decomposition is another decomposition algorithm on the basis of a solid mathematical model [17]. Sparse transform method is based on that fact the seismic data can be compressed in a transformed

The associate editor coordinating the review of this manuscript and approving it for publication was Jinming Wen.

domain, in which the useful signal is delineated by high-amplitude coefficients while the noise is represented by low-amplitude ones. Thus, a thresholding function can be applied in the transformed domain in order to remove those low-amplitude coefficients corresponding to noise, then the rest of coefficients are transformed back to the time domain to reconstruct the useful signal. Widely used sparse transforms consist of Fourier transform, curvelet transform [18], [19], S-transform [20], [21], seislet transform [22], [23], shearlet transform [24], dreamlet transform [25], wavelet transform [26], [27], synchrosqueezing transform [28], etc. Rand based method including rank reduction and low-rank approximation is also common approach in seismic data processing community, which contains singular spectrum analysis [29], multichannel singular spectrum analysis [30], damped singular spectrum analysis [31], multistep damped singular spectrum analysis [32], and low-rank matrix approximation [33], [34]. In the rank reduction strategy, the denoised signal can be recovered by reducing the rank of the matrix obtained from the noisy seismic data. In the second strategy, the noisy seismic data is decomposed into a low-rank matrix and a sparse matrix, in which the low-rank matrix is viewed as the useful signal while the sparse matrix as the noise, thus, one can obtain the filtered signal by implementing an inverse transform on the low-rank matrix. In addition to the aforementioned classic denoising algorithms, other methods also include mean and median filters [35], time-frequency peak filtering [36], and so on.

Recently, a new adaptive signal analysis algorithm called high-order synchrosqueezing transform (FSSTH) was introduced in [37]. FSSTH produces a highly focused time-frequency map for a wide range of multicomponent signal by calculating more accurate instantaneous frequency based on higher order approximations both for the amplitude and the phase, and FSSTH can reconstruct the modes making up the input signal with a high precision [37]. Currently, FSSTH has successfully been applied to machine fault diagnosis [38], [39], seismic time-frequency analysis [40], and the analysis of a transient gravitational-wave signal [37]. However, the applications in seismic noise suppression are seldom reported.

In this paper, we propose a novel method for seismic random noise suppression that incorporate the FSSTH and the sparse low-rank estimation for seismic data. First of all, the FSSTH of the noisy seismic data is computed to produce a sparse time-frequency matrix. Then, a low-rank matrix and a sparse one are estimated based on solving a convex relaxation optimization problem by using robust principle component analysis (RPCA), which is a classical low-rank matrix recovery algorithm. Finally, we implement an inverse FSSTH on the obtained low-rank matrix to reconstruct the denoised signal in the time domain. The contributions of the paper can be summarized as below: (1) we first integrate the superior sparse property of FSSTH and the low-rank estimation algorithm to suppress seismic random noise, (2) our method shows the excellent potential in seismic random noise removal compared to the conventional denoising approaches.

This paper is structured as follows: in Section II, we present the key principle of our method. Next, the experimental results on both synthetic data and real field datasets are shown in Section III. The discussion regarding the parameter selection is given in Section IV. Finally, Section V concludes this paper.

II. THEORY

A. HIGH-ORDER SYNCHROSQUEEZING TRANSFORM

The high-order synchrosqueezing transform (FSSTH) is a new generalization of the short-time Fourier-based synchrosqueezing transform (FSST), which was first proposed by Thakur and Wu [41]. The key idea of such a technique is to sharpen the time-frequency map by computing more accurate instantaneous frequency by means of higher order approximations in both amplitude and phase [37]. FSSTH achieves an excellent concentration and reconstruction for a wider range of AM-FM signal modes.

Considering an AM-FM signal s:

$$s(t) = A(t)\, e^{i2\pi\psi(t)}. \tag{1}$$

where $\psi(t)$ and $A(t)$ are the instantaneous phase and amplitude, respectively.

The short-time Fourier transform (STFT) regarding the signal s with a window function g can be represented as:

$$V_s^g(t,\zeta) = \int s(\tau) g^*(\tau - t)\, e^{-i2\pi\zeta(\tau - t)} d\tau. \tag{2}$$

where t is the time variable and ζ is the frequency variable, g^* is the complex conjugate with respect to g.

Now, let $\omega_s(t,\zeta)$ denote the instantaneous frequency with respect to t and ζ.

$$\omega_s(t,\zeta) = R\left\{ \frac{\partial_t V_s^g(t,\zeta)}{i2\pi V_s^g(t,\zeta)} \right\}, \tag{3}$$

where $R\{\bullet\}$ means to extract the real part of a complex number. ∂_t means taking the derivative regarding t.

Thus, the conventional FSST is defined as below:

$$T_s^{g,\gamma}(t,\omega) = \frac{1}{g^*(0)} \int_{\{\zeta, |V_s^g(t,\zeta)| > \gamma\}} V_s^g(t,\zeta)\, \delta(\omega - \omega_s(t,\zeta)) d\zeta. \tag{4}$$

where γ is the threshold, δ is the Dirac distribution.

FSST has a solid theoretical foundation. However, the application of such a technique is still limited to a class of signal characterized by 'slowly varying' instantaneous frequency. This is because the weak frequency modulation hypothesis regarding the modes is imposed in the algorithm.

To deal with this issue, Pham and Meignen (2017) improved existing FSST algorithm by calculating more accurate instantaneous frequency through high-order Taylor expansion about the amplitude and the phase of a given signal.

The Taylor expansion regarding the signal s in Eq. (1) for τ close to t is expressed as:

$$s(\tau) = \exp\left(\sum_{n=0}^{M} \frac{\left[\log(A)\right]^{(n)}(t) + i2\pi\psi^{(n)}(t)}{n!}(\tau - t)^n\right). \tag{5}$$

where $X^{(n)}(t)$ is the nth derivative of X with respect to t.

Substituting Eq. (5) into Eq. (2), we obtain

$$\begin{aligned} &V_s^g(t,\zeta) \\ &= \int s(\tau + t) g^*(\tau) e^{-i2\pi\zeta\tau} d\tau \\ &= \int \exp\left(\sum_{n=0}^{M} \frac{\left[\log(A)\right]^{(n)}(t) + i2\pi\psi^{(n)}(t)}{n!}\tau^i\right) \\ &\qquad g^*(\tau) e^{-i2\pi\zeta\tau} d\tau. \end{aligned} \tag{6}$$

And, Eq. (3) can be rewritten as:

$$\begin{aligned} \omega_s(t,\zeta) = &\frac{\left[\log(A)\right]'(t)}{i2\pi} + \psi'(t) \\ &+\sum_{n=2}^{M} \frac{\left[\log(A)\right]^{(n)}(t) + i2\pi\psi^{(n)}(t)}{i2\pi\,(n-1)!} \frac{V_s^{t^{n-1}g}(t,\zeta)}{V_s^g(t,\zeta)} \end{aligned} \tag{7}$$

Now, let us introduce a frequency modulation operator $q_{\zeta,s}^{[n,M]}$:

$$q_{\zeta,s}^{[n,M]} = \frac{\left[\log(A)\right]^{(n)}(t) + i2\pi\psi^{(n)}(t)}{i2\pi\,(n-1)!}, \tag{8}$$

Then, the Mth-order local complex instantaneous frequency $\omega_{\zeta,s}^{[M]}$ can be expressed by:

$$\omega_{\zeta,s}^{[M]}(t,\zeta) = \begin{cases} \omega_s(t,\zeta) + \sum_{n=2}^{M} q_{\zeta,s}^{[n,M]}(\xi,t) \\ \left(-x_{n,1}(t,\zeta)\right) \\ V_s^g(t,\zeta) \\ \neq 0,\ \partial_\zeta x_{k,k-1}(t,\zeta) \neq 0\,(k \geq 2) \\ \omega_s(t,\zeta) \\ otherwise \end{cases} \tag{9}$$

Finally, substituting $\omega_{\zeta,s}^{[M]}(t,\zeta)$ for $\omega_s(t,\zeta)$ in Eq. (4), we obtain the FSSTH, namely:

$$\begin{aligned} &T_{M,s}^{g,\gamma}(t,\omega) \\ &= \frac{1}{g^*(0)} \int_{\{\zeta,|V_s^g(t,\zeta)|>\gamma\}} V_s^g(t,\zeta)\,\delta\left(\omega - \omega_{\zeta,s}^{[M]}(t,\zeta)\right) d\zeta. \end{aligned} \tag{10}$$

Meanwhile, the mode of the input signal can be reconstructed by:

$$s_k(t) \approx \int_{\{\omega,|\omega-\varphi_k(t)|<\sigma\}} T_{M,s}^{g,\gamma}(t,\omega) d\omega. \tag{11}$$

where σ is the compensation factor and $\varphi_k(t)$ is the estimation of $\psi_k'(t)$.

B. ROBUST PRINCIPAL COMPONENT ANALYSIS

In this paper, we utilize the robust principal component analysis (RPCA) algorithm [42] to decompose the noisy seismic data into a low-rank matrix and a sparse matrix, which can be described as below:

$$d = L + S. \tag{12}$$

where d denotes the seismic data corrupted by random noise, and L and S are the low-rank matrix and the sparse matrix, respectively.

The low-rank matrix L can be obtained by the following constrained optimization problem.

$$\min rank(L) + \mu\|S\|_0, \quad subject\ to\ d = L + S. \tag{13}$$

where $rank(L)$ denotes the rank of the low-rank matrix, $\|\bullet\|_0$ is the l_0 norm of a matrix, μ is a factor and $\mu > 0$ in which it is employed to balance the two components in Eq. (13).

It is worth noting that the aforementioned optimization problem is NP-hard and non-convex [43]. In order to cope with this issue, one can transform the Eq. (13) into a convex relaxation optimization problem by using l_1 norm and nuclear norm, namely:

$$\min \|L\|_* + \mu\|S\|_1, subject\ to\ d = L + S. \tag{14}$$

where $\|\bullet\|_*$ and $\|\bullet\|_1$ denote the nuclear norm and the l_1 norm of a matrix, respectively.

In fact, there are several algorithms to solve Eq. (14) [43]. In this paper, we adopt the exact augmented Lagrange multiplier algorithm:

$$\begin{aligned} F(L,S,Y,\sigma) = &\|L\|_* + \mu\|S\|_1 + \langle Y, d - L - S\rangle \\ &+ \frac{\sigma}{2}\|d - L - S\|_F^2. \end{aligned} \tag{15}$$

where Y is the Lagrange multiplier, σ is a penalty term that is utilized to ensure the convergence of Eq. (15), $\|\bullet\|_F$ denotes the Frobenius norm.

In the process of solving Eq. (15), the Y and S are firstly fixed, then the L is calculated until the F is minimized.

$$L_{n+1} = \arg\min_L F(L, S_{n+1}, Y_n, \sigma_n). \tag{16}$$

Next, the L and Y are fixed, and the S is obtained when the F is minimized.

$$S_{n+1} = \arg\min_S F(L_{n+1}, S, Y_n, \sigma_n). \tag{17}$$

where n and $n+1$ denote the nth and $(n+1)$th iterations, respectively.

Finally, Y and σ are updated based on Eq. (18) and Eq. (19):

$$Y_{n+1} = Y_n + \sigma(d - L_{n+1} - S_{n+1}). \tag{18}$$

$$\sigma_{n+1} = \varepsilon\sigma_n. \tag{19}$$

where ε is a constant and $\varepsilon > 1$.

After multiple iterations, Eq. (15) is minimized, and then the optimal low-rank matrix and sparse matrix are obtained, which correspond to the useful signal and noise, respectively.

Algorithm 1 The Proposed Algorithm

Input: noisy seismic data d
Output: denoised seismic data $\widehat{d}$

1: Predefinition: γ, ϖ, μ, N and Y
2: Iterate on $n = 1, \cdots, N$
3: **for** each noisy seismic trace n **do**
4: Estimation of the TFR regarding the seismic trace n via Eq. (10)
5: Separation of the amplitude and phase spectrums
6: Extract the low-rank matrix and sparse one via Eq. (16) and Eq. (17)
7: Transform back the low-rank matrix into the time domain via Eq. (11)
8: **end for**
9: Rearrange the denoised seismic trace n along the spatial direction
10: **return** denoised seismic data $\widehat{d}$

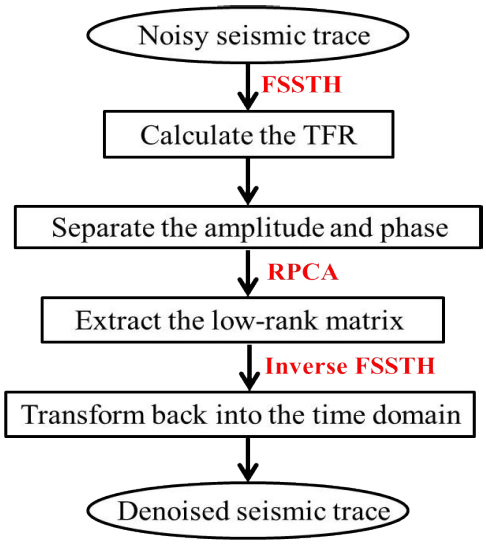

FIGURE 1. The denoising framework for seismic data.

C. PROPOSED ALGORITHM

The seismic signal and noise will be sparse in the time-frequency domain through the FSSTH. Then, we can implement the RPCA algorithm on time-frequency representation of a noisy seismic trace to extract a low-rank matrix and a sparse matrix that are corresponding to the useful signal and noise, respectively. Finally, the denoised signal is recovered by back-transforming the obtained low-rank matrix to the time domain using the inverse FSSTH. The complete process of the proposed algorithm is summarized in Algorithm 1. Figure 1 illustrates the denoising framework. The specific steps are summarized as below:

1) Compute the TFR of a noisy seismic trace based on the FSSTH algorithm.

2) Separate the amplitude and phase spectrums of the obtained TFR.

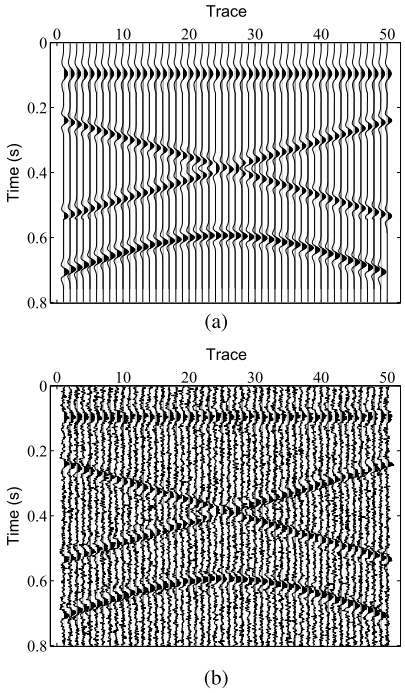

FIGURE 2. The synthetic data composed of a horizontal event, two steep linear events and a hyperbolic one. (a) Original noise-free synthetic data. (b) noisy synthetic data with a SNR of 2 dB.

3) Decompose the amplitude spectrum of TFR by means of RPCA algorithm to extract the low-rank matrix and the sparse one.

4) View the low-rank matrix as the denoised amplitude spectrum.

5) Transform the low-rank matrix back into the time domain to obtain the denoised seismic trace by using the inverse FSSTH.

6) Implement the steps (1)-(5) repeatedly until all seismic traces are finished.

In the aforementioned algorithm, γ is the threshold, ϖ is the window parameter, μ is the regularization parameter, N is the length of the seismic trace, and Y is the augmented Lagrange parameter.

III. EXAMPLES

A. EVALUATION OF DENOISING PERFORMANCE

In this section, we use several examples including a synthetic data and two real field datasets to verify the effectiveness of our proposed method. In order to numerically evaluate the denoising performance, the signal to noise ratio (SNR) and mean squared error (MSE) are defined as follows:

$$SNR = 10\log_{10}\left(\frac{\|s\|_2}{\|\hat{s} - s\|_2}\right). \tag{20}$$

$$MSE = \frac{1}{M}\sum_{m=1}^{M}\left[\hat{s}\,(m) - s\,(m)\right]^2. \tag{21}$$

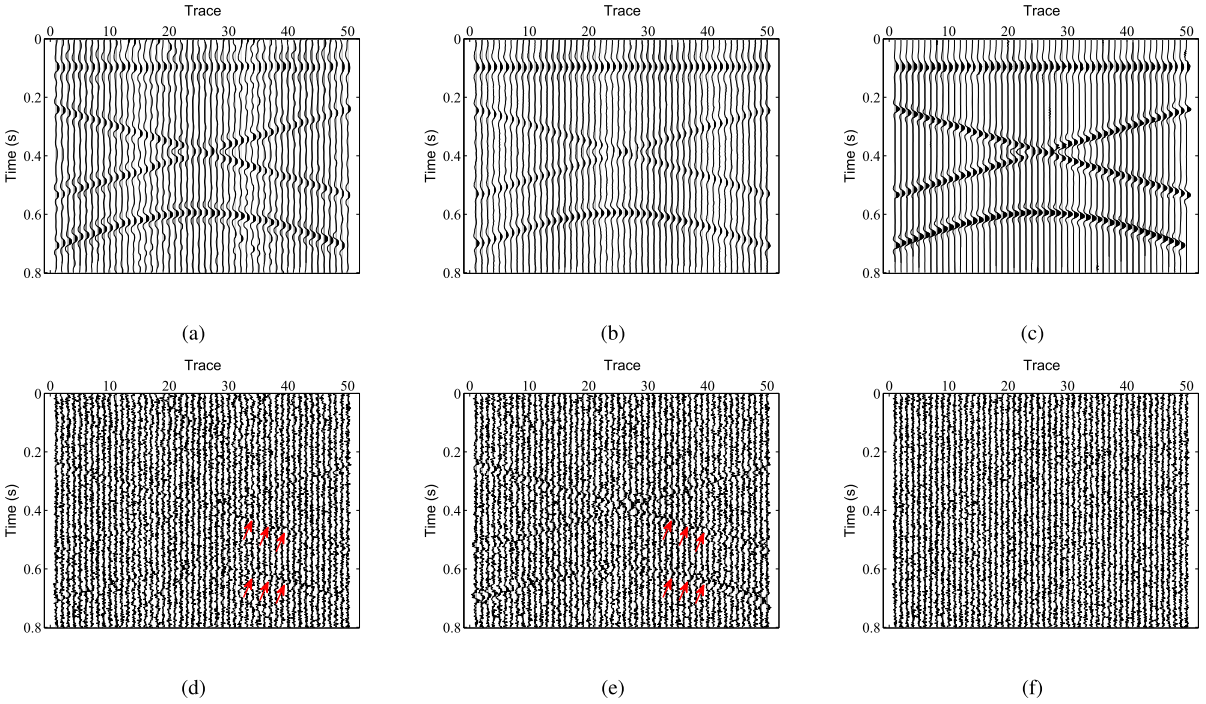

FIGURE 3. Denoised results using (a) $f-x$ SSA, (b) $f-x$ deconvolution, and (c) the proposed method. Difference sections between noisy and denoised data for (d) $f-x$ SSA, (e) $f-x$ deconvolution, and (f) the proposed method.

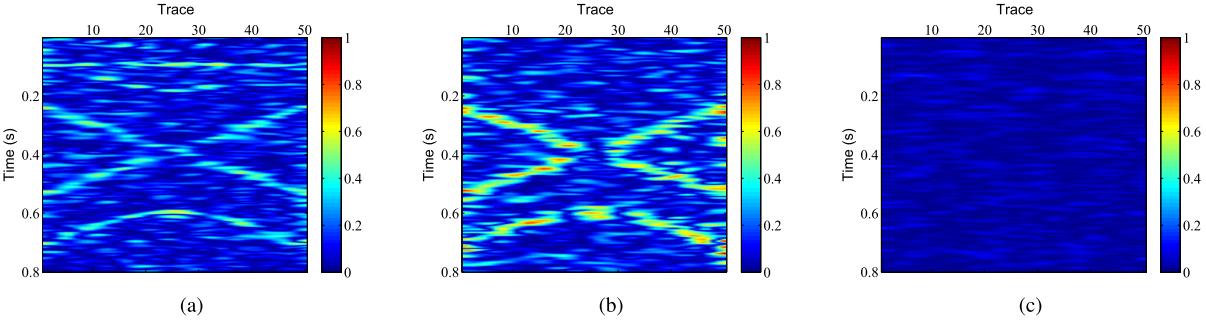

FIGURE 4. Comparison of local similarity maps. (a) $f-x$ SSA, (b) $f-x$ deconvolution, and (c) the proposed method.

where s or $s(m)$ is the noise-free signal, $\hat{s}$ or $\hat{s}(m)$ is the denoised signal, and M is the length of a signal.

B. SYNTHETIC DATA

We first utilize a synthetic example to demonstrate the performance of our method. Figure 2(a) shows the synthetic data, which includes a horizontal event, two steep linear events and a hyperbolic one. This data has 50 traces with the sampling interval of 2 ms, and the total time is 0.8 s. The noisy synthetic data with a SNR of 2dB is presented in Figure 2(b), which is severely contaminated by random noise. In this synthetic example, our method has been implemented with a regularization parameter of 0.0225. For $f-x$ SSA, the rank parameter is selected as five because of the presence of nonlinear events in the data. In the $f-x$ deconvolution method, the filter length is 15 and the required frequency range is from 1 to 120 Hz.

The denoised results based on the the $f-x$ SSA, the $f-x$ deconvolution, and the proposed method are shown in Figures 3(a), (b), and (c), respectively, and the corresponding noise sections are exhibited in Figures 3(d), (e), and (f), respectively. It can be clearly seen that both methods, the $f-x$ SSA and $f-x$ deconvolution, are able to suppress most of the random noise, but the useful seismic reflections can also be found in the removed noise sections in Figures 3(d) and (e), which means such approaches indeed do harm to some useful signals. Furthermore, there exists some significant residual noise in the filtered result by $f-x$ SSA (see Figure 3(a)). In contrast, the proposed method not only suppresses noise effectively, but also prevents the useful seismic information leakage well, as shown in Figures 3(c) and (f). Figure 4 shows

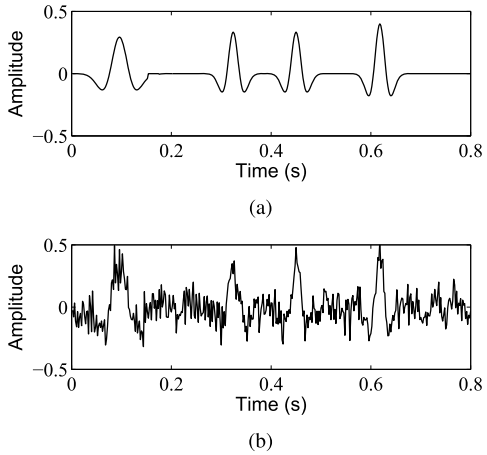

FIGURE 5. Clean trace 15 (a) and noisy one (b).

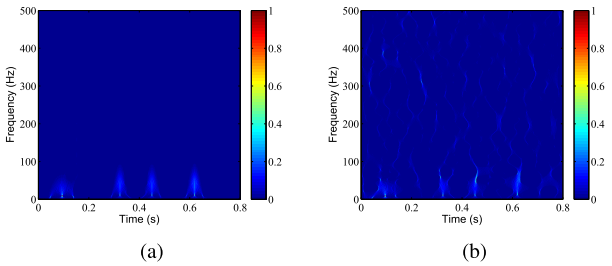

FIGURE 6. Sparse TFR of clean trace 15 (a) and noisy one (b) using FSSTH.

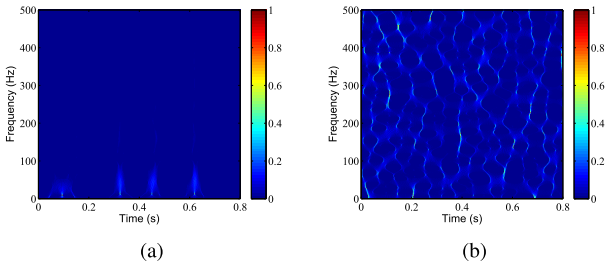

FIGURE 7. Decomposition result via the RPCA. (a) low-rank component and (b) sparse component.

the comparison of local similarity maps based on the denoised data and the removed noise. It is very obvious that Figure 4(c) has the lowest similarity, which indicates that the proposed method has the least signal leakage.

Now, we take the trace 15 from the noise-free synthetic data and the noisy version, which are plotted in Figures 5(a) and (b), respectively, and perform the FSSTH on them. Figures 6(a) and (b) show the time-frequency representations of the above-mentioned two signals, respectively. We utilize the RPCA algorithm to decompose the time-frequency matrix of the noisy seismic signal into the low-rank component and sparse component as shown in Figures 7(a) and (b), respectively. Then, the estimated low-rank and sparse components are transformed back into the time domain via the inverse transform of FSSTH in order to obtain the denoised seismic signal and noise, which are

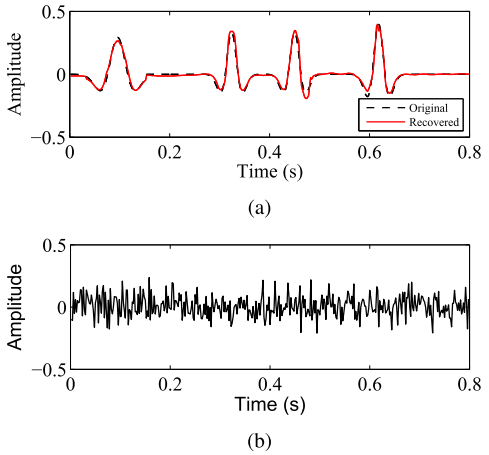

FIGURE 8. (a) Recovered (red line) and original (dashed black line). (b) estimated noise.

presented in Figures 8(a) and (b), respectively. As can be clearly seen, there is no appreciable difference between the recovered signal and the original one. Through the proposed method, we have improved the SNR of synthetic data from 2 dB to 8.5 dB.

For further performance evaluation regarding the denoising algorithms, we have calculated the amplitude spectrums of noise-free data, noisy data, and filtered data using the $f-x$ SSA, $f-x$ deconvolution, and the proposed method. The results are shown in Figure 9. One clearly sees the proposed algorithm is capable of removing random noise effectively and retrieve the amplitude spectrum of the original signal well. However, the other two methods cannot completely attenuate random noise (see the blue boxes in Figures 9(c) and (d)), and the $f-x$ SSA damages some low-frequency contents in the seismic signal to some extent (see the red box in Figure 9(c)).

In addition, we also compute the SNR and MSE of the results based on the three denoising methods in Figure 10 by changing the input SNR. It is obvious that the proposed algorithm always outperforms the other two methods in terms of SNR and MSE.

C. FIELD DATA

To verify the performance of the proposed method in real seismic data, we use a 100-traces shot data shown in Figure 11, wherein there are 400 time samples in each trace and the sampling interval is 2 ms. In this shot gather example, we set the regularization parameter to 0.025 in our method, the rank parameter for $f-x$ SSA is 18, and the desired frequency band regarding the $f-x$ deconvolution is from 1 to 120 Hz and the filter length is 10. The filtered results using the $f-x$ SSA, the $f-x$ deconvolution, and the proposed method are shown in Figures 12(a), (c), and (e), respectively. The corresponding removed noise sections are illustrated in Figures 12(b), (d), and (f), respectively. It can be observed that although the $f-x$ SSA and $f-x$ deconvolution remove amounts of random noise, there are still

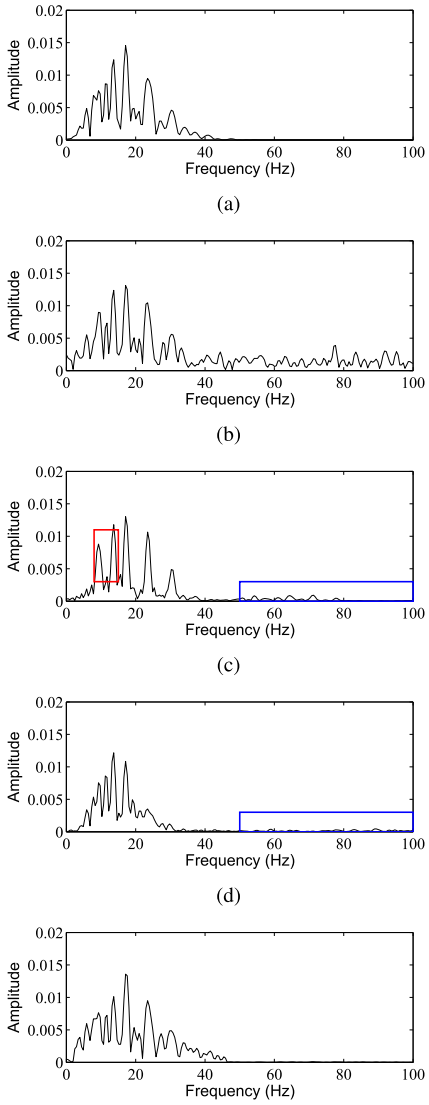

FIGURE 9. Amplitude spectrum of (a) original data, (b) noisy data, and denoised data using the (c) $f-x$ SSA, (d) $f-x$ deconvolution, and (e) the proposed method.

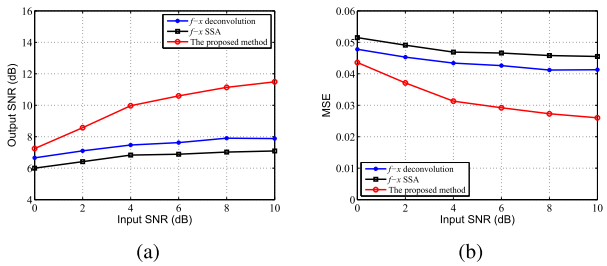

FIGURE 10. Output SNR (a) and MSE (b) comparison of the three methods for various input SNR.

some seismic reflections left in the removed noise (see Figures 12(b) and (d)). By contrast, the proposed method performs clearly better, the random noise is effectively suppressed and the seismic signals are well preserved.

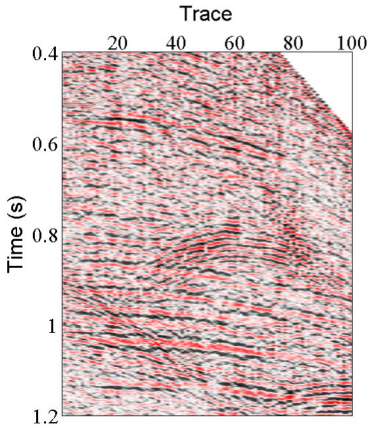

FIGURE 11. Noisy real shot data.

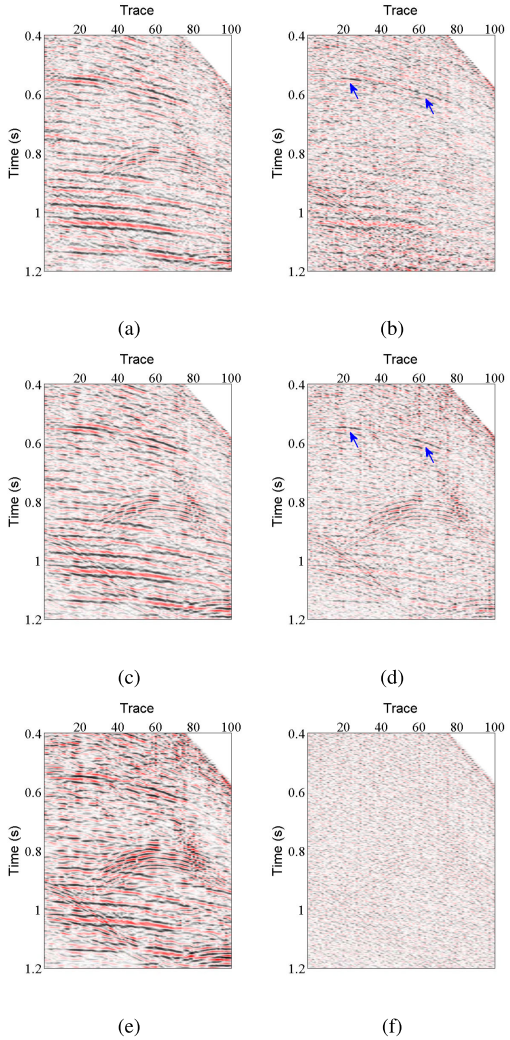

FIGURE 12. Denoised results of shot data using (a) $f-x$ SSA, (c) $f-x$ deconvolution, and (e) the proposed algorithm, respectively. (b), (d), and (f) are the removed noise corresponding to the three methods.

For better visualization and comparison, we have zoomed in one area of interest ranging from 0.4 to 0.8 s, which is shown in Figure 13. As shown on the figure, the

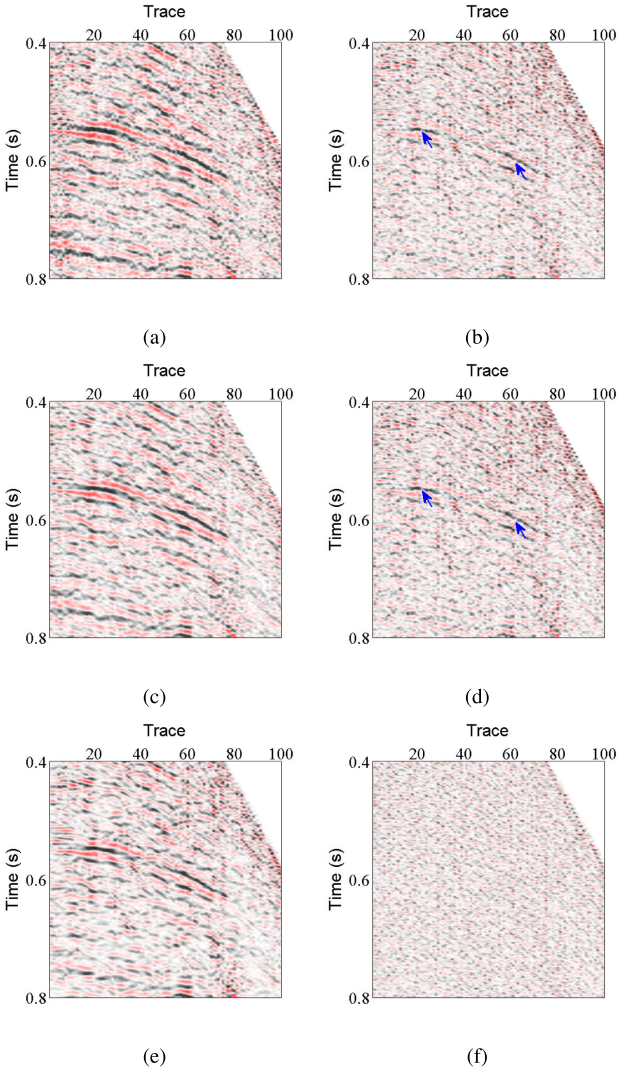

FIGURE 13. Zoomed denoised results and removed noise using (a) (b) $f-x$ SSA, (c) (d) $f-x$ deconvolution, and (e) (f) the proposed algorithm, respectively.

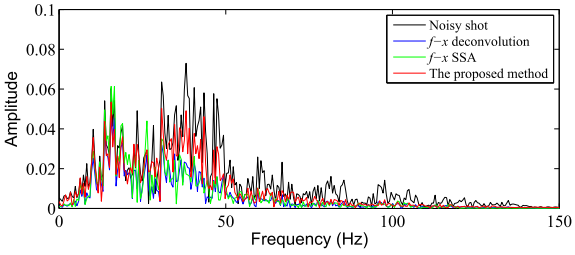

FIGURE 14. Amplitude spectrums of the aforementioned methods.

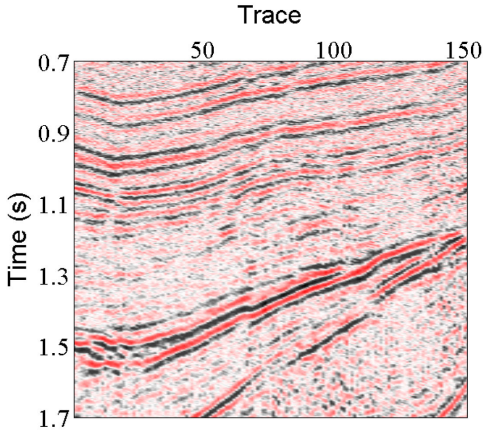

FIGURE 15. Noisy post-stack data.

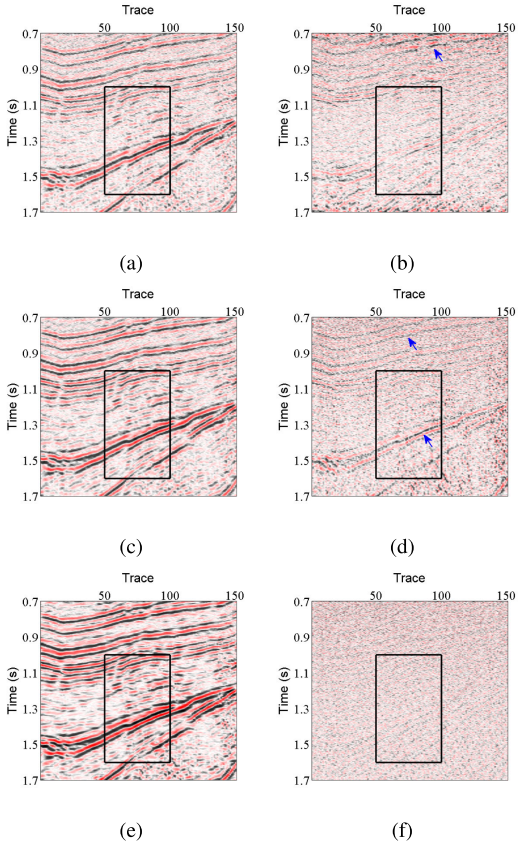

FIGURE 16. Denoised results based on (a) $f-x$ SSA, (c) $f-x$ deconvolution, and (e) the proposed algorithm, respectively. (b), (d), and (f) are the corresponding removed noise regarding the three methods.

proposed algorithm does better than the other two methods in improving the SNR of original shot data and preserving the amplitude of the seismic reflections.

Additionally, we also have computed the amplitude spectrums regarding the aforementioned methods in Figure 14. It can be clearly seen that the proposed method can effectively attenuate random noise and retrieve the amplitude spectrum of the seismic signal well, but the $f-x$ SSA and $f-x$ deconvolution cannot properly preserve the useful seismic reflections.

The second field data example is a post-stack data. It is shown in Figure 15, which has 150 traces and 500 samples per trace with a sampling interval of 2 ms. For the proposed method, the regularization parameter is chosen as 0.025. In the $f-x$ SSA method, we set the rank parameter to 20. The desired frequency range is still from

1 to 120 Hz, but the length of filter is selected as 12 for the $f-x$ deconvolution. The denoised results using the $f-x$ SSA, $f-x$ deconvolution, and the proposed algorithm are given in Figures 16(a), (c), and (e), respectively. Figures 16(b), (d), and (f) are the resulting noise sections. From these figures, we can observe that although a large amount of random noise has successfully been suppressed, some seismic reflection events also have already been removed using the $f-x$ SSA and $f-x$ deconvolution (see Figures 16(b) and (d)). By comparison, the proposed method has greatly improved the SNR of original post-stack data, the seismic reflections have become clearer and the seismic structures of reflection events are well preserved (see Figures 16(e) and (f)).

Similarly, for better visualization and comparison, the zoomed-in versions regarding the results marked by a rectangle are shown in Figure 17. It is obvious that the proposed method does a better job in noise reduction and seismic signal preservation compared with the $f-x$ SSA and the $f-x$ deconvolution. In addition, the amplitude spectrums also indicate the superior performance of the proposed method (see Figure 18).

IV. DISCUSSION

In this paper, we have presented a robust method for denoising seismic data, in which it first transforms the noisy seismic trace into the sparse time-frequency domain using the FSSTH, then, the low-rank matrix and sparse matrix are extracted via the RPCA algorithm. Since the proposed method is operated based on trace by trace, its performance might not be affected by the geological complexity of seismic data.

Based on the above-mentioned theory, we can obtain the denoised signal from the low-rank matrix of time-frequency representation of the input seismic data. Thus, it is crucial to extract the low-rank matrix accurately. It is noteworthy that there are two key parameters, the regularization parameter μ and the augmented Lagrange parameter Y, in the RPCA algorithm that need to be selected properly. We test the effect of the regularization parameter and the augmented Lagrange parameter on the output SNR for the synthetic trace in Figure 5(b), which are shown in Figures 19(a) and (b), respectively. As can be observed from figures, the proposed method is sensitive to the regularization parameter value, however, it seems to be relatively insensitive to the augmented Lagrange parameter value. Therefore, we should do several trials to select the optimal regularization parameter value in real case. In addition, it should be noted that a larger value of the augmented Lagrange parameter will increase the computational cost. Hence, considering the performance of noise suppression and computational efficiency, we should take a compromise solution.

The $f-x$ SSA and $f-x$ deconvolution are two classical denoising algorithms for seismic data. For the first algorithm, the target rank is an important parameter, which has a direct influence on noise attenuation and signal preservation.

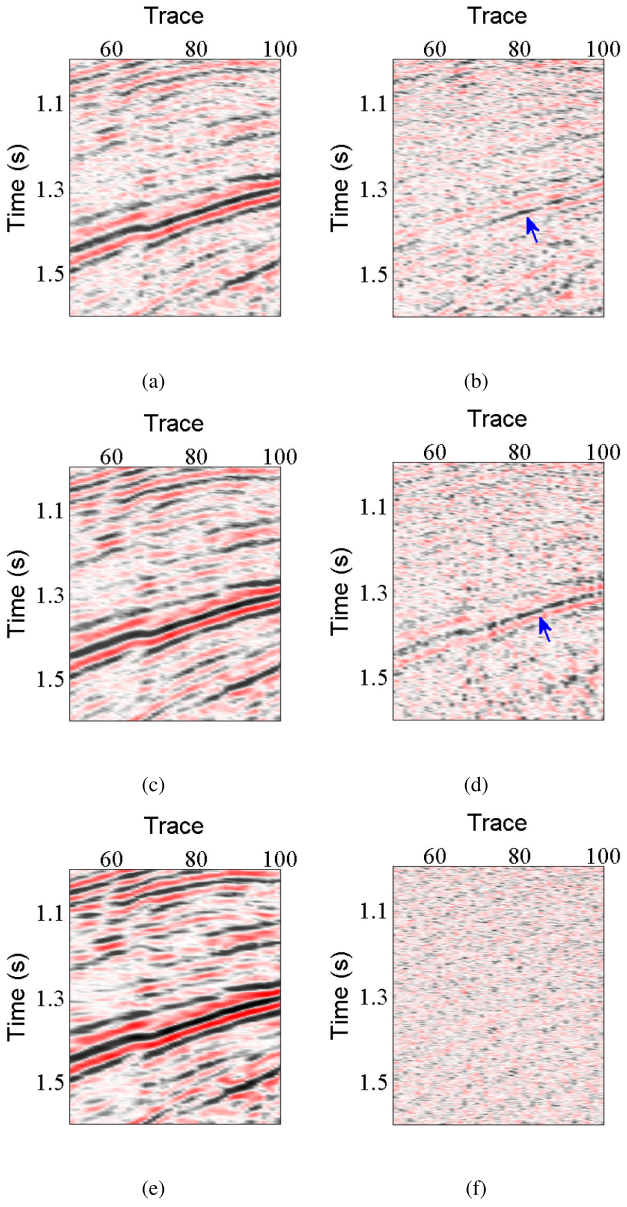

FIGURE 17. Zoomed results and corresponding noise using (a) (b) $f-x$ SSA, (c) (d) $f-x$ deconvolution, and (e) (f) the proposed algorithm, respectively.

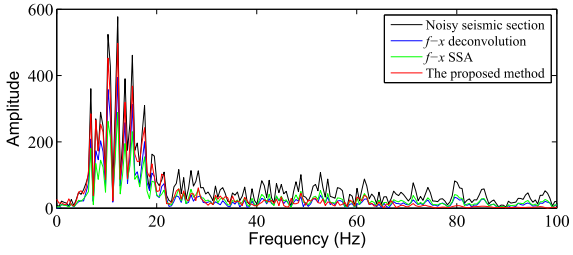

FIGURE 18. Amplitude spectrums of the aforementioned methods.

The larger the rank parameter, the weaker the noise attenuation, and vice versa. For the second algorithm, the noise suppression depends on two input parameters, namely the

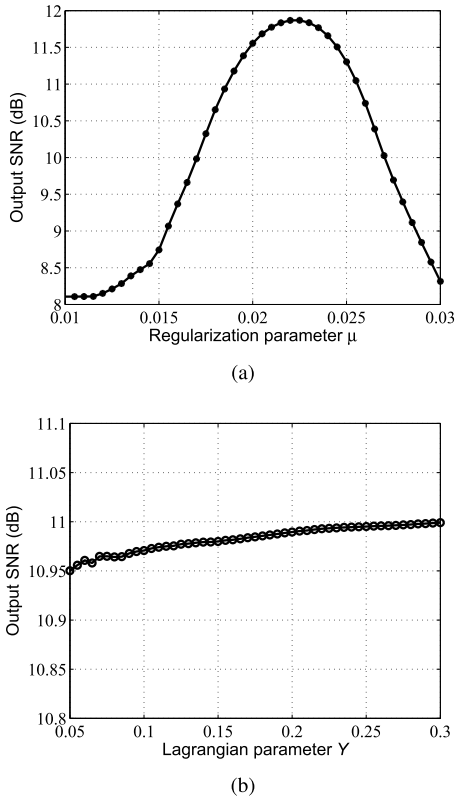

FIGURE 19. Output SNR versus different regularization parameter values (a) and different augmented Lagrange parameter values (b), respectively.

length of operator and the processing frequency. In practice, several trials should be done for different parameters so that we can obtain the satisfactory result.

V. CONCLUSION

We have proposed a robust random noise suppression method for seismic data in the time-frequency domain. In this paper, we utilize the FSSTH to transform the noisy seismic data to the sparse time-frequency domain. Then, the low-rank matrix and sparse matrix are estimated by decomposing the time-frequency map via the RPCA algorithm. Finally, the denoised signal can be recovered by performing the inverse transform of FSSTH on the obtained low-rank matrix. The experimental results on a synthetic data and two field data examples demonstrate the superiority of our approach. By using the proposed method, the SNR of the seismic data is greatly improved and the useful signals are well preserved in contrast to the $f-x$ SSA and $f-x$ deconvolution methods, which renders the technique highly promising for seismic processing.

ACKNOWLEDGMENT

The authors would like to thank associate editor Dr. Jinming Wen and two anonymous reviewers for their constructive comments that improve the manuscript greatly.

REFERENCES

[1] L. Yang, W. Chen, W. Liu, B. Zha, and L. Zhu, "Random noise attenuation based on residual convolutional neural network in seismic datasets," *IEEE Access*, vol. 8, pp. 30271–30286, 2020.
[2] M. Zhang, Y. Liu, and Y. Chen, "Unsupervised seismic random noise attenuation based on deep convolutional neural network," *IEEE Access*, vol. 7, pp. 179810–179822, 2019.
[3] Y. Zhang, H. Lin, Y. Li, and H. Ma, "A patch based denoising method using deep convolutional neural network for seismic image," *IEEE Access*, vol. 7, pp. 156883–156894, 2019.
[4] Y. Sang, J. Sun, X. Meng, H. Jin, Y. Peng, and X. Zhang, "Seismic random noise attenuation based on PCC classification in transform domain," *IEEE Access*, vol. 8, pp. 30368–30377, 2020.
[5] L. L. Canales, "Random noise reduction," in *Proc. 54th Annu. Int. Meeting, SEG, Expanded Abstr.*, Jan. 1984, pp. 525–527.
[6] R. Abma and J. Claerbout, "Lateral prediction for noise attenuation by t-x and f-x techniques," *Geophysics*, vol. 60, no. 6, pp. 1887–1896, 1995.
[7] Y. Chen and J. Ma, "Random noise attenuation by f-x empirical mode decomposition predictive filtering," *Geophysics*, vol. 79, no. 3, pp. V81–V91, 2014.
[8] Y. Wang, "Random noise attenuation using forward-backward linear prediction," *J. Seismic Exploration*, vol. 8, no. 2, pp. 133–142, 1999.
[9] N. E. Huang, Z. Shen, S. R. Long, M. C. Wu, H. H. Shih, Q. Zheng, N.-C. Yen, C. C. Tung, and H. H. Liu, "The empirical mode decomposition and the Hilbert spectrum for nonlinear and non-stationary time series analysis," *Proc. Roy. Soc. London A, Math., Phys. Eng. Sci.*, vol. 454, no. 1971, pp. 903–995, Mar. 1998.
[10] W.-L. Hou, R.-S. Jia, H.-M. Sun, X.-L. Zhang, M.-D. Deng, and Y. Tian, "Random noise reduction in seismic data by using bidimensional empirical mode decomposition and shearlet transform," *IEEE Access*, vol. 7, pp. 71374–71386, 2019.
[11] Z. Wu and N. E. Huang, "Ensemble empirical mode decomposition: A noise-assisted data analysis method," *Adv. Adapt. Data Anal.*, vol. 1, no. 1, pp. 1–41, Jan. 2009.
[12] M. E. Torres, M. A. Colominas, G. Schlotthauer, and P. Flandrin, "A complete ensemble empirical mode decomposition with adaptive noise," in *Proc. IEEE Int. Conf. Acoust., Speech Signal Process. (ICASSP)*, May 2011, pp. 4144–4147.
[13] M. Sun, Z. Li, Z. Li, Q. Li, Y. Liu, and J. Wang, "A noise attenuation method for weak seismic signals based on compressed sensing and CEEMD," *IEEE Access*, vol. 8, pp. 71951–71964, 2020.
[14] W. Chen, Y. Chen, J. Xie, S. Zu, and Y. Zhang, "Multiples attenuation using trace randomization and empirical mode decomposition," in *Proc. 86th Annu. Int. Meeting, SEG, Expanded Abstr.*, 2016, pp. 4498–4502.
[15] K. Dragomiretskiy and D. Zosso, "Variational mode decomposition," *IEEE Trans. Signal Process.*, vol. 62, no. 3, pp. 531–544, Feb. 2014.
[16] W. Liu and Z. Duan, "Seismic signal denoising using $f-x$ variational mode decomposition," *IEEE Geosci. Remote Sens. Lett.*, vol. 17, no. 8, pp. 1313–1317, Aug. 2020.
[17] G. Wu, S. Fomel, and Y. Chen, "Data-driven time-frequency analysis of seismic data using regularized nonstationary autoregression," in *Proc. 86th Annu. Int. Meeting, SEG, Expanded Abstr.*, 2016, pp. 1700–1705.
[18] E. Candès, L. Demanet, D. Donoho, and L. Ying, "Fast discrete curvelet transforms," *Multiscale Model. Simul.*, vol. 5, no. 3, pp. 861–899, Jan. 2006.
[19] F. J. Herrmann, U. Böniger, and D. J. Verschuur, "Non-linear primary-multiple separation with directional curvelet frames," *Geophys. J. Int.*, vol. 170, no. 2, pp. 781–799, Aug. 2007.
[20] R. G. Stockwell, L. Mansinha, and R. P. Lowe, "Localization of the complex spectrum: The S transform," *IEEE Trans. Signal Process.*, vol. 44, no. 4, pp. 998–1001, Apr. 1996.
[21] C. R. Pinnegar and D. W. Eaton, "Application of the S transform to prestack noise attenuation filtering," *J. Geophys. Res., Solid Earth*, vol. 108, no. B9, pp. 1–10, Sep. 2003.
[22] S. Fomel and Y. Liu, "Seislet transform and seislet frame," *Geophysics*, vol. 75, no. 3, pp. V25–V38, May 2010.
[23] Y. Chen and S. Fomel, "EMD-seislet transform," in *Proc. 85th Annu. Int. Meeting, SEG, Expanded Abstr.*, 2015, pp. 4775–4778.
[24] D. Kong and Z. Peng, "Seismic random noise attenuation using shearlet and total generalized variation," *J. Geophys. Eng.*, vol. 12, no. 6, pp. 1024–1035, Dec. 2015.
[25] B. Wang, R.-S. Wu, X. Chen, and J. Li, "Simultaneous seismic data interpolation and denoising with a new adaptive method based on dreamlet transform," *Geophys. J. Int.*, vol. 201, no. 2, pp. 1180–1192, 2015.
[26] S. Sinha, P. S. Routh, P. D. Anno, and J. P. Castagna, "Spectral decomposition of seismic data with continuous-wavelet transform," *Geophysics*, vol. 70, no. 6, pp. P19–P25, Nov. 2005.

[27] W. Liu and W. Chen, "Recent advancements in empirical wavelet transform and its applications," *IEEE Access*, vol. 7, pp. 103770–103780, 2019.
[28] I. Daubechies, J. Lu, and H.-T. Wu, "Synchrosqueezed wavelet transforms: An empirical mode decomposition-like tool," *Appl. Comput. Harmon. Anal.*, vol. 30, no. 2, pp. 243–261, Mar. 2011.
[29] R. Vautard, P. Yiou, and M. Ghil, "Singular-spectrum analysis: A toolkit for short, noisy chaotic signals," *Phys. D, Nonlinear Phenomena*, vol. 58, nos. 1–4, pp. 95–126, Sep. 1992.
[30] V. Oropeza and M. Sacchi, "Simultaneous seismic data denoising and reconstruction via multichannel singular spectrum analysis," *Geophysics*, vol. 76, no. 3, pp. V25–V32, May 2011.
[31] Y. Chen, D. Zhang, Z. Jin, X. Chen, S. Zu, W. Huang, and S. Gan, "Simultaneous denoising and reconstruction of 5-D seismic data via damped rank-reduction method," *Geophys. J. Int.*, vol. 206, no. 3, pp. 1695–1717, Sep. 2016.
[32] D. Zhang, Y. Chen, W. Huang, and S. Gan, "Multi-step reconstruction of 3D seismic data via an improved MSSA algorithm," in *Proc. CPS/SEG Beijing Int. Geophys. Conf. Expo., SEG, Expanded Abstr.*, 2016, pp. 745–749.
[33] M. A. Nazari Siahsar, S. Gholtashi, A. R. Kahoo, H. Marvi, and A. Ahmadifard, "Sparse time-frequency representation for seismic noise reduction using low-rank and sparse decomposition," *Geophysics*, vol. 81, no. 2, pp. V117–V124, Mar. 2016.
[34] R. Anvari, M. A. N. Siahsar, S. Gholtashi, A. R. Kahoo, and M. Mohammadi, "Seismic random noise attenuation using synchrosqueezed wavelet transform and low-rank signal matrix approximation," *IEEE Trans. Geosci. Remote Sens.*, vol. 55, no. 11, pp. 6574–6581, Nov. 2017.
[35] Y. Liu, C. Liu, and D. Wang, "A 1D time-varying median filter for seismic random, spike-like noise elimination," *Geophysics*, vol. 74, no. 1, pp. V17–V24, Jan. 2009.
[36] A. Kahoo, "Random noise suppression from seismic data using time frequency peak filtering," in *Proc. 71st Annu. Int. Conf. Exhib., EAGE, Extended Abstr.*, 2014, p. cp-127.
[37] D. Pham and S. Meignen, "High-order synchrosqueezing transform for multicomponent signals analysi—With an application to gravitationalwave signal," *IEEE Trans. Signal Process.*, vol. 65, no. 12, pp. 3168–3178, Jun. 2017.
[38] W. Liu, W. Chen, and Z. Zhang, "A novel fault diagnosis approach for rolling bearing based on high-order synchrosqueezing transform and detrended fluctuation analysis," *IEEE Access*, vol. 8, pp. 12533–12541, 2020.
[39] X. Tu, Y. Hu, F. Li, S. Abbas, Z. Liu, and W. Bao, "Demodulated high-order synchrosqueezing transform with application to machine fault diagnosis," *IEEE Trans. Ind. Electron.*, vol. 66, no. 4, pp. 3071–3081, Apr. 2019.
[40] W. Liu, S. Cao, Z. Wang, K. Jiang, Q. Zhang, and Y. Chen, "A novel approach for seismic time-frequency analysis based on high-order synchrosqueezing transform," *IEEE Geosci. Remote Sens. Lett.*, vol. 15, no. 8, pp. 1159–1163, Aug. 2018.
[41] G. Thakur and H.-T. Wu, "Synchrosqueezing-based recovery of instantaneous frequency from nonuniform samples," *SIAM J. Math. Anal.*, vol. 43, no. 5, pp. 2078–2095, Jan. 2011.
[42] X. Dong, T. Zhong, and Y. Li, "New suppression technology for low-frequency noise in desert region: The improved robust principal component analysis based on prediction of neural network," *IEEE Trans. Geosci. Remote Sens.*, vol. 58, no. 7, pp. 4680–4690, Jul. 2020.
[43] Y. Liu, X. Gao, Q. Gao, L. Shao, and J. Han, "Adaptive robust principal component analysis," *Neural Netw.*, vol. 119, pp. 85–92, Nov. 2019.

PINGPING BING received the Ph.D. degree in geophysics from the China University of Petroleum (Beijing), Beijing, China, in 2012. She is currently a Lecturer with Changsha Medical University. Her research interests include optimization algorithm, signal analysis and model prediction, and deep learning.

WEI LIU received the B.E. degree in exploration geophysics from the China University of Petroleum (East China), Qingdao, China, in 2006, the M.S. degree in exploration geophysics from the China University of Petroleum (Beijing), Beijing, China, in 2009, and the Ph.D. degree in geological resources and geological engineering from the China University of Petroleum (Beijing), in 2016. He is currently working as a Lecturer with the Beijing University of Chemical Technology. His research interests include signal analysis and processing, seismic data processing and interpretation, and mechanical fault diagnosis.

ZHIHUA ZHANG received the B.E. degree in safety science and engineering from the North University of China, in 2018. He is currently pursuing the M.E. degree with the Beijing University of Chemical Technology. His research interests include signal analysis, deep learning, and intelligent fault diagnosis.